Available online at www.sciencedirect.com
SCIENCE DIRECT®
Bioorganic & Medicinal Chemistry 14 (2006) 3681–3690
Bioorganic & Medicinal Chemistry

Hydroxyl-terminated peptidomimetic inhibitors of neuronal nitric oxide synthase

Bessie N. A. Mbadugha,[a,†,‡] Jiwon Seo,[a,‡] Haitao Ji,[a] Pavel Martásek,[c,§] Linda J. Roman,[c,¶] Thomas M. Shea,[c,§] Huiying Li,[d,e,f,‖] Thomas L. Poulos[d,e,f,‖] and Richard B. Silverman[a,b,*]

[a]*Department of Chemistry, Center for Drug Discovery and Chemical Biology, Northwestern University, Evanston, IL 60208-3113, USA*
[b]*Department of Biochemistry, Molecular Biology and Cell Biology, Northwestern University, Evanston, IL 60208-3113, USA*
[c]*Department of Biochemistry, The University of Texas Health Science Center, San Antonio, TX 78384-7760, USA*
[d]*Department of Molecular Biology and Biochemistry, The Center in Chemical and Structural Biology, University of California, Irvine, CA 92697-3900, USA*
[e]*Department of Chemistry, The Center in Chemical and Structural Biology, University of California, Irvine, CA 92697-3900, USA*
[f]*Department of Physiology and Biophysics, The Center in Chemical and Structural Biology, University of California, Irvine, CA 92697-3900, USA*

Received 16 November 2005; revised 11 January 2006; accepted 12 January 2006
Available online 9 February 2006

Abstract—The X-ray structure of previously studied dipeptidomimetic inhibitors bound in the active site of neuronal nitric oxide synthase (nNOS) presented a possibility for optimizing the strength of enzyme–inhibitor interactions as well as for enhancing bioavailability. These desirable properties may be attainable by replacement of the terminal amino group of the parent compounds (**1**–**6**) with a hydroxyl group (**11**–**13**, and **18**–**20**). The hypothesized effect would be twofold: first, a change from a positively charged amino group to a neutral hydroxyl group might afford more drug-like character and blood–brain barrier permeability to the inhibitors; second, as suggested by docking studies, the incorporated hydroxyl group might displace an active site water molecule with which the terminal amino group of the original compounds indirectly hydrogen bonds. In vitro activity assays of the hydroxyl-terminated analogs (**11**–**13** and **18**–**20**) showed greater than an order of magnitude *increase* in K_i values (decreased potency) relative to the amino-terminated compounds. These experimental data support the importance to enzyme binding of a potential electrostatic interaction relative to a hydrogen bonding interaction.

1. Introduction

Three isoforms of nitric oxide synthase (neuronal or nNOS, endothelial or eNOS, and inducible or iNOS) have been identified as catalysts in the production of nitric oxide (NO), via the NADPH- and O_2-dependent oxidation of L-arginine.[1] Nitric oxide serves as a second messenger for a number of physiological and pathological processes including mediation of neurotransmission and regulation of smooth muscle relaxation.[2,3] An overproduction of NO from the neuronal isoform (nNOS) has been implicated in strokes, migraine headaches, Parkinson's disease, and Alzheimer's disease, while NO overproduction from the inducible isoform (iNOS) has been associated with tissue damage, inflammation, rheumatoid arthritis, and the onset of colitis.[1,2] Blocking the

Keywords: Nitric oxide synthase; Neuronal nitric oxide synthase; Peptidomimetic; Enzyme inhibitors; Hydroxyl-terminated; Computer modeling.
* Corresponding author. Tel.: +1 847 491 5653; fax: +1 847 491 7713; e-mail: Agman@chem.northwestern.edu
† Present address: Department of Chemistry and Biochemistry, St. Mary's College of Maryland, St. Mary's City, MD 20686, USA.
‡ Carried out the synthetic and enzymatic experiments in this study.
§ Developed the eNOS overexpression system in *E. coli* and the purification of eNOS.
¶ Developed the overexpression system for nNOS in *E. coli* and the purification of the nNOS.
‖ Obtained the crystal structures of inhibitors bound to nNOS.

0968-0896/$ - see front matter © 2006 Elsevier Ltd. All rights reserved.
doi:10.1016/j.bmc.2006.01.044

localized excess production of NO has been identified as a potential means of treating these diseases. However, because of the critical role that eNOS-generated NO plays in vascular regulation, the potential pharmaceutical utility of NOS inhibitors is restricted to the selective inhibition of the neuronal or inducible isoforms.[4]

Recent strategies toward the development of nNOS-specific inhibitors have been comprehensively summarized in a recent review article.[5] Our research group has conducted extensive investigations of a number of N^{ω}-nitroarginine-containing dipeptide compounds (Fig. 1) that have shown promise as selective inhibitors of nNOS;[6–10] (4*S*)-*N*-(4-amino-5-[aminoethyl]aminopentyl)-*N*′-nitroguanidine (**4**) exhibits outstanding potency for nNOS inhibition (K_i = 120 nM) as well as high selectivity over eNOS (greater than 2600-fold) and iNOS (325-fold). The correlation of amine side-chain length to the potency and selectivity of inhibitors **1**–**6** (Table 1) may stem from steric and/or electrostatic effects, as the basic amino nitrogen could interact with the enzyme-binding site as both an ionic moiety and as a hydrogen bond donor. A crystal structure of the reduced dipeptide (4*S*)-*N*-(4-amino-5-[aminoethyl]aminopentyl)-*N*′-nitroguanidine (**4**) bound to nNOS shows the side-chain amino group involved in a hydrogen bonding interaction through a water molecule (Wat5 in Fig. 2A) with the propionate group of the heme (D) moiety of the enzyme (Fig. 2).[11,12] The significance of this indirect hydrogen bond is suggested by the detection of a similar indirect hydrogen bond interaction, also mediated by Wat5 (Fig. 2B), between the amino group of the dipeptide inhibitor **7** and the heme (D) carboxylate group. These data suggest that changing the terminal amino group to a terminal hydroxyl group could produce a similar binding effect, while lowering the charge of the molecule by one cation, which may enhance bioavailability.

Therefore, it became of interest to evaluate the effect on potency upon substitution of the basic amino group of both series of inhibitors with a hydroxyl moiety. This proposed structural modification could potentially afford hydrogen bonding without the electrostatic interaction associated with the amino moiety (which is protonated at physiological pH) as well as increase the lipophilicity of the target drug for more favorable blood–brain barrier crossing potential as measured by increased log *D*. Furthermore, a hydroxyl group attached to a sufficiently long chain may be able to displace the active site water molecule (Wat5) for a direct hydrogen bond with the enzyme, yielding a stronger inhibitor–enzyme binding interaction, which may ultimately increase the potency of nNOS inhibition.

Table 1. In vitro assay data for dipeptide[8] and dipeptidomimetic inhibitors[10]

Compound	K_i (μM)			Selectivity	
	nNOS	iNOS	eNOS	n/e	n/i
1	0.54	100	199	368	185
2	0.46	118	213	463	256
3	0.35	108	70	200	308
4	0.12	39	314	2617	325
5	0.29	73	524	1807	252
6	0.46	123	411	893	267
7	0.13	25	200	1538	192

The K_i values represent at least duplicate measurements; standard deviations of ±8–12% were observed.

2. Results

2.1. AutoDock calculations

Docking simulations were carried out as described by Ji et al.[13] with AutoDock 3.0, using the crystal structure of dipeptide (4*S*)-*N*-(4-amino-5-[aminoethyl]aminopentyl)-*N*′-nitroguanidine (**4**) bound to nNOS (PDB ID: 1p6i) to define the binding pocket. The appropriate ligand targets were built in SYBYL 6.8 by modifying the molecular structure of **4**, which was extracted from the crystal structure. Energy minimizations were performed following both the addition of polar hydrogen atoms and partial atom charge calculations by the Gasteiger–Marsilli method.[14] Appropriate atom types were specified and labeled for physiological conditions, and ligand chirality was inspected. An atom fit between the ligand and the active site conformation of **4** was performed, and the center was defined. The grid box dimensions were set at 31 Å × 28 Å × 31 Å, and the spacing was set to 0.375 Å. Default parameters as described in detail previously[13] were used, and 100 docked conformations were yielded. A visual comparison of the superposition of the guanidino moiety of the calculated conformations and that of **4** served as a preliminary identification of appropriate structures. Conformations were then further evaluated based on their total docking energies.

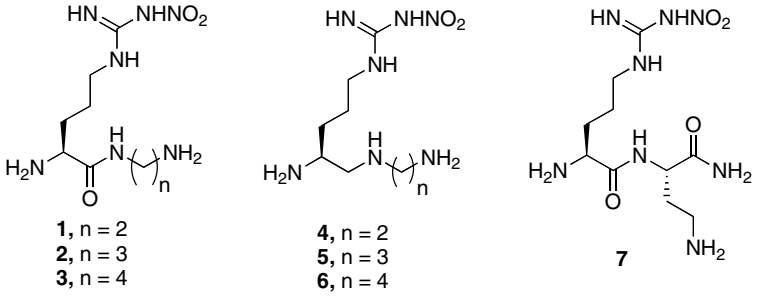

Figure 1. Structures of dipeptide and dipeptidomimetic inhibitors previously studied; K_i values and selectivities are shown in Table 1.

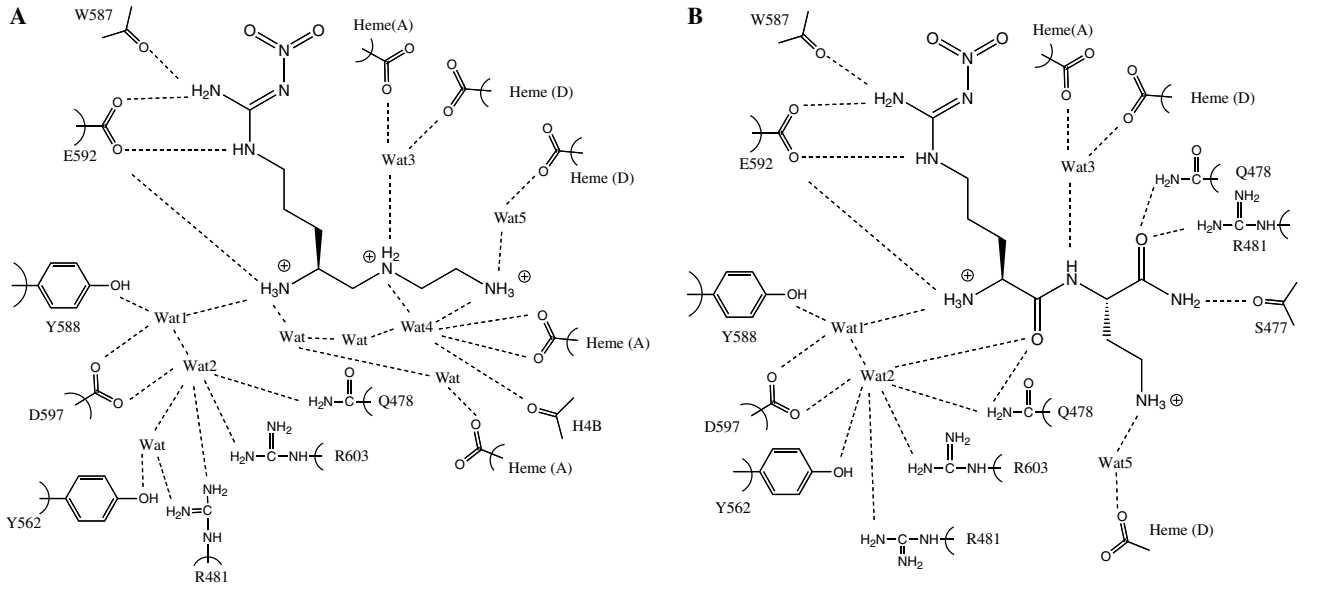

Figure 2. Schematic drawings representing the interactions between inhibitor **4** (A) or inhibitor **7** (B) and nNOS.

Table 2. $\log D_{7.4}$ values for the amino and hydroxyl compounds

Compound	$\log D_{7.4}$
1	−5.44
2	−5.38
3	−5.13
4	−5.88
5	−5.54
6	−5.27
11	−2.56
12	−2.30
13	−2.33
18	−4.25
19	−5.50
20	−3.98

2.2. log $D_{7.4}$ calculations

log D values for the inhibitors were calculated at pH 7.4[15]; the results are summarized in Table 2.

2.3. Chemistry

The amido derivatives (**11**–**13**) were prepared using standard peptide coupling procedures of the amino alcohols with Boc-nitro-L-arginine (Scheme 1). The synthetic protocol used in the preparation of the reduced amide peptidomimetics[10] was readily adaptable for the synthesis of the hydroxyl analogs (Scheme 2). N^{α}-(*tert*-Butoxycarbonyl)-L-nitroargininal (**14**) was prepared as described previously[10] using a protocol that involved a Weinreb amide as the key intermediate. Pyridine-borane complex[16] was effective for the reductive amination of the amino alcohols to **14**. It was shown earlier that racemization does not occur during reductive amination.[10] Purification of the amido and amino adducts was achieved by column chromatography, and TFA treatment yielded the deprotected final products **18**–**20**. Further purification of the deprotected products using preparative HPLC was carried out prior to conducting the assays to achieve greater than 95% purity of the compounds.

2.4. Enzyme inhibition

Following the preparation and purification of the six target molecules, in vitro assays were conducted to assess the biological activity of the proposed inhibitors. The three NOS isoforms, which have high sequence identity in different sources, were obtained as recombinant enzymes overexpressed in *Escherichia coli*. The assay exploits the fact that nitric oxide produced by L-Arg

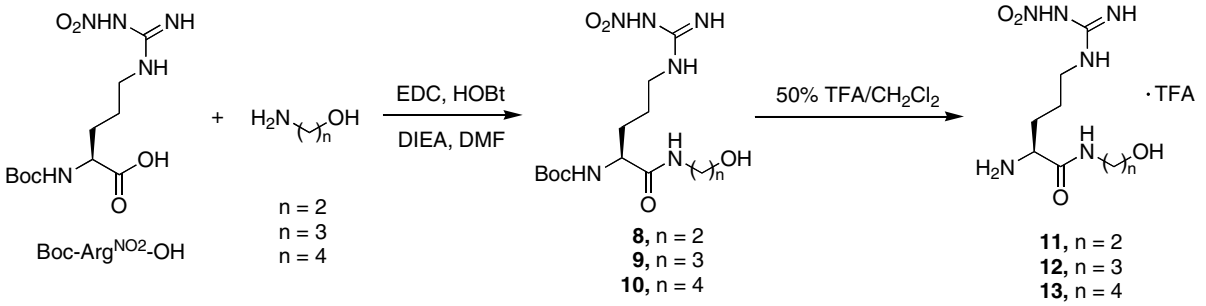

Scheme 1.

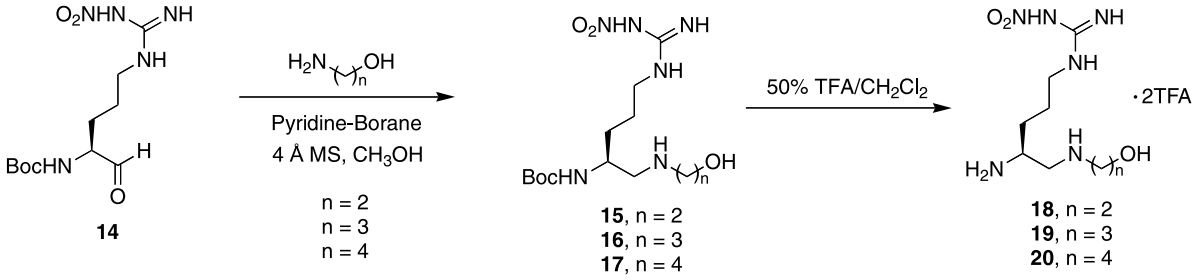

Scheme 2.

Table 3. Nitric oxide synthase (NOS) inhibition and selectivities of hydroxyl-terminated analogues

Compound	Apparent K_i (μM)			Selectivity	
	nNOS	iNOS	eNOS	n/e	n/i
11	8.3	181	165	20	22
12	3.1	645	449	145	208
13	12.3	373	398	32	30
18	15.6	391	534	34	25
19	39.9	853	750	19	21
20	13.1	318	147	11	24

The K_i values represent single measurements with 5–6 data points and correlation coefficients of 0.945–0.998.

and NOS forms a complex with oxyhemoglobin to yield methemoglobin, which has a maximum absorbance at 401 nm. Monitoring the initial rate of methemoglobin production upon enzyme addition to the assay mixture thus permits the determination of the IC_{50}. Measurements were performed using a series of inhibitor concentrations that allowed for data points on either side of the IC_{50}; the reported values are not based on extrapolations. The results are shown in Table 3.

3. Discussion

The three NOS isoforms have 50% sequence homology but differ in terms of their localization and regulatory properties. The active sites of the three isozymes are almost identical; each has a similar affinity for its common natural substrate L-arginine. Extensive research by a number of investigators has revealed that inhibition selectivity is attainable with various ligands, including nitroarginine derivatives.[5] The availability of X-ray crystallography data has opened avenues for further design of potentially potent and selective inhibitors by revealing slight differences in isozyme active sites through structural comparison and analysis.[13]

Based on the mode of action of inhibitors **4** and **7** with nNOS, as shown in Figure 2, the indirect hydrogen bond between the terminal amino group, through an active site water molecule to the enzyme, appears to be a critical interaction because it exists in both structures.[11,12] The distribution of the key structural waters in the nNOS active site in three-dimensional space is illustrat-

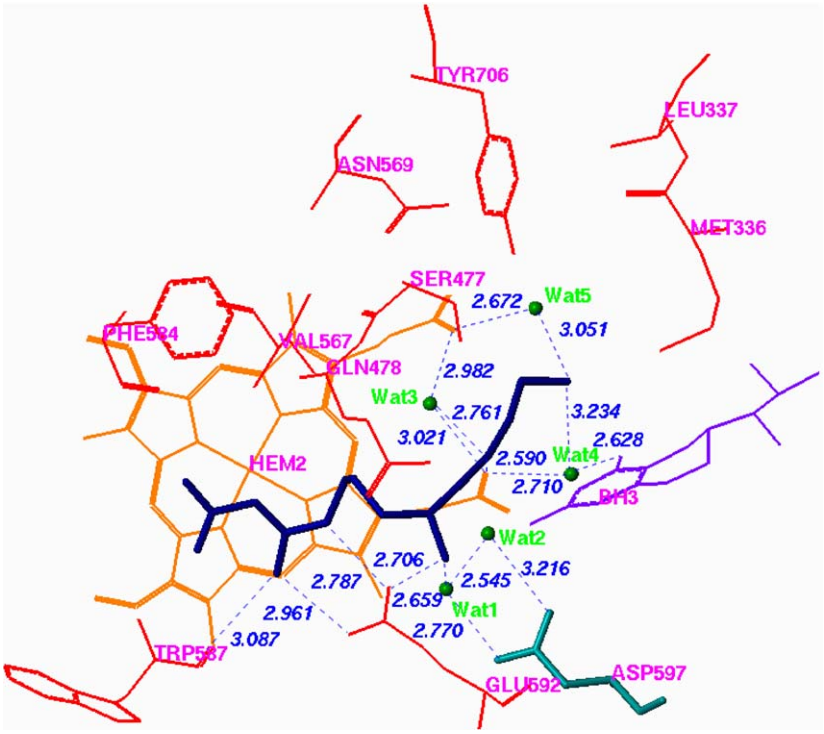

Figure 3. The distribution of the structural waters in the crystal structure and the binding mode of inhibitor **4** in complex with rat nNOS.

Table 4. The distances of the main hydrogen bonds involved in the binding of inhibitor **4** with rat nNOS

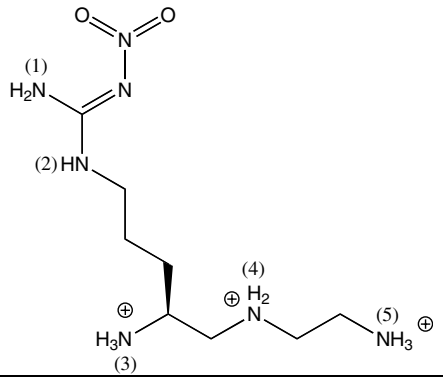

Residues	Distance (Å)
N1(4)–CO(W587)	3.087
N1(4)–CO(E592)	2.961
N2(4)–CO(E592)	2.787
N3(4)–CO(E592)	2.706
N3(4)–O(Wat1)	2.659
O(Wat1)–O(Wat2)	2.545
O(Wat1)–CO(D597)	2.770
O(Wat2)–CO(D597)	3.216
N4(4)–CO(Heme A)	2.590
N4(4)–O(Wat3)	2.761
CO(Heme A)–O(Wat3)	3.021
CO(Heme A)–O(Wat4)	2.710
O(Wat4)–CO(H_4B)	2.628
N5(4)–O(Wat4)	3.234
N5(4)–O(Wat5)	3.051
O(Wat3)–CO(Heme D)	2.982
CO(Heme D)–O(Wat5)	2.672

Wat1–Wat5 are the five structural water molecules observed in the crystal structure. Heme A and D correspond to heme propionate side chain A and heme propionate side chain D, respectively.

ed in Figure 3, and the distances of the main hydrogen bonds involved in the binding of inhibitor **4** to rat nNOS are given in Table 4. The potential displacement of the active site water molecule (Wat5 in Fig. 3) by substitution of the amino group with a hydroxyl group for a direct hydrogen bond between the ligand and enzyme might afford a stronger binding interaction. In addition, we can anticipate a favorable entropic gain by liberating a tightly bound water molecule from the protein to the bulk solvent. The estimated energy gain is reported to be as high as 2 kcal/mol.[17] A classical example provided by Lam et al.[18] demonstrated that the inclusion of a structural water molecule in their inhibitor design afforded cyclic urea HIV protease inhibitors with increased potency and bioavailability relative to the lead molecules. The proposed structural modification in the current work, namely to replace the terminal amino group with a hydroxyl group, would also yield a less charged molecule that might be better suited for blood–brain barrier permeability.

AutoDock calculations of **4**, **12**, and **18** bound to the active site of nNOS were performed using the coordinates from the X-ray structure of **4** bound to nNOS. Two goals were set for the docking calculations: to determine whether the hydroxyl analogs can mimic the interaction of amine compound **4** or **7** and to see if the hydroxyl group of the proposed inhibitors can occupy the position of the structural water, affording direct hydrogen bonding to the enzyme. To test the efficiency and capability of AutoDock for the docking of the dipeptide inhibitors to nNOS, **4** was docked into the active site of nNOS resulting in the accurate prediction of the binding mode as shown in Figure 4. Two different conformations of **12** provided by AutoDock calculations are depicted in Figure 5A, where the blue structure is the crystallographic binding conformation of **4**. The cyan conformation of **12** indicates that **12** can mimic the interaction of **4** with nNOS with distances from the oxygen atom of the terminal hydroxyl group of **12** to heme propionate A and to structural Wat4 of 2.628 and 2.816 Å, respectively. Alternatively, the green conformation of **12** in Figure 5A indicates that **12** can replace structural Wat5 to form a hydrogen bond directly to the heme propionate D. The distance between the hydroxyl group of **12** and the heme propionate D is 2.902 Å. Docking compound **18** into the active site of nNOS also indicates that the terminal hydroxyl group of **18** can mimic the terminal amino group of **4** (Fig. 5B). The side chain of **18** is one carbon shorter than that of **12** but is capable of hydrogen bonding to the heme propionate A and to structural Wat4. The distances from the oxygen atom of the terminal hydroxyl group of **18** to the oxygen atom of heme propionate A and to the oxygen atom of the structural Wat4 are 2.587 and 2.886 Å, respectively.

The results in Table 3, as compared to those summarized in Table 1, do not indicate an enhancement of inhibition potency or selectivity upon substitution of the hydroxyl group for the amino moiety. The docking calculations suggested that the terminal hydroxyl group could occupy the position of the structural water and afford direct hydrogen bonding to the enzyme. However, this apparently does not occur because a substantial diminution of potency and selectivity was observed for all of the hydroxyl-substituted compounds. These data suggest that the terminal amino group (or possibly related functional group) promotes inhibitor binding to the enzyme. Although the nNOS potencies of the target molecules are two orders of magnitude lower than those of the corresponding amino-terminated analogs (see **18** vs **4** and **19** vs **5**), the general trend of greater nNOS potency relative to iNOS or eNOS still prevails, although the selectivity is considerably lower. This diminished selectivity results from the greater loss in potency for nNOS than that for iNOS or eNOS. The hydroxyl-terminated chain does not appear to elicit as strong an interaction with the enzyme as does the amino-terminated chain. The charge of the amino group may act as a 'lock' to hold the inhibitor into the substrate-binding site. The in vitro assay data suggest that this interaction is stronger than the potential displacement of the water molecule with a hydroxyl-terminated chain. Variation in chain length does not appear to have a significant impact on the potencies of either family of compounds.

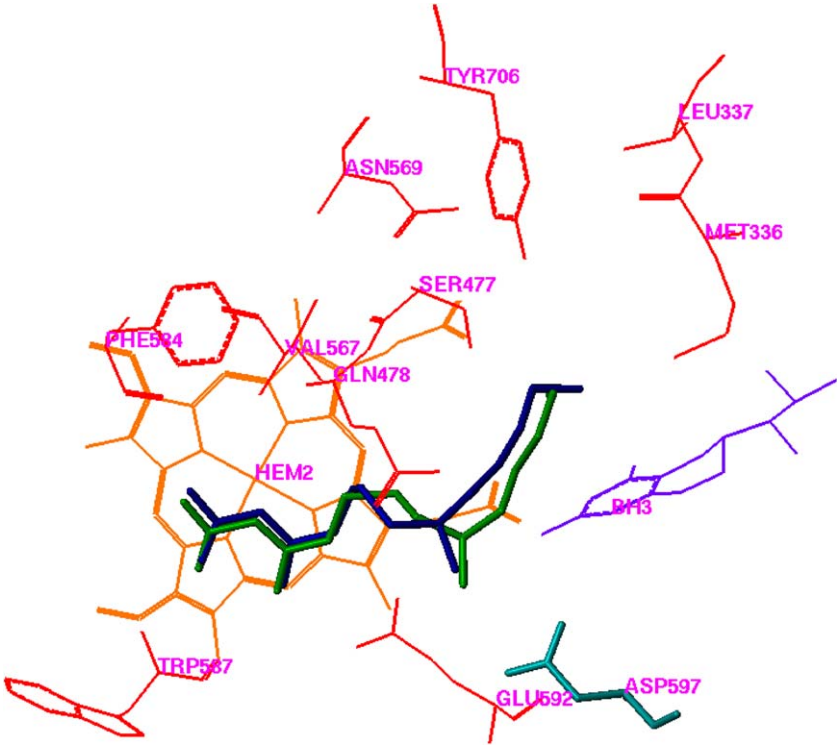

Figure 4. Superposition of crystallographic and docked conformations of **4** in nNOS. The blue conformation is the crystallographic binding orientation; the green structure is the predicted docking orientation.

4. Conclusions

Conversion of the terminal amino group of previously studied peptidomimetic inhibitors to a hydroxyl group does not provide the significant enhancement of inhibitor potency or selectivity hypothesized. Preliminary docking experiments suggested a potential displacement of an active site water molecule by an incorporated hydroxyl group to afford direct ligation of the compounds to the enzyme via a hydrogen bond. However, substitution of the amino moiety with a hydroxyl group resulted in a 100-fold reduction of in vitro activity, perhaps due to the loss of a potential long-range electrostatic interaction between the terminal amino group of inhibitor **4** and the heme carboxylate.

5. Experimental

5.1. General methods

Docking calculations were performed using AutoDock3.0 and SYBYL 6.8 software on a Silicon Graphics workstation. ^{1}H and ^{13}C NMR spectra were obtained with a Varian INOVA 500 or 400 MHz NMR spectrometer. Chemical shifts are reported as δ values in parts per million with the $CHCl_3$ and HOD resonance peaks set at 7.27 and 4.80 ppm, respectively. E. Merck pre-coated silica gel 60 F254 plates were used for thin-layer chromatography (TLC), with visualization accomplished with a ninhydrin spray reagent or with a UV–vis lamp. Flash chromatography was performed with Sorbent Technologies 250 mesh silica gel. Preparative HPLC (Waters Prep LC 4000 System) was carried out using an Alltech Econosil 10 μ C_{18} (250 × 22 mm) column with an isocratic solvent system of either 25:75 methanol/water (containing 0.1% TFA) for compounds **18** and **19** or 30:70 methanol/water (containing 0.1% TFA) for **11**–**13**, and **20** at a flow rate of 10 mL/min, detecting at 290 nm with a Waters 2487 Dual lambda absorbance detector. Fractions containing pure compound were concentrated in vacuo and the residue was lyophilized. pH measurements were conducted with an Orion Research model 701 pH meter. Mass spectroscopy analyses were carried out at the University of Illinois, Urbana-Champaign using a Micromass Quattro spectrometer. Elemental analyses were performed by Atlantic Microlab Inc. The NOS assays were conducted with a Perkin-Elmer Lambda 10 UV–vis spectrophotometer.

5.2. Reagents and materials

Boc-nitro-L-arginine was purchased from Advanced ChemTech, Inc. NADPH, calmodulin, and human ferrous hemoglobin were purchased from Sigma Chemical Co. Tetrahydrobiopterin was obtained from Alexis Biochemicals. All organic solvents and all other chemicals not specified above were purchased from Fisher Scientific and Aldrich, respectively.

5.3. General procedure for the synthesis of dipeptidomimetic analogs 11–13

The general protocol followed for coupling the amino alcohols to Boc-Arg^{NO_2}-OH to yield amides **11**–**13** involved the addition of the appropriate amino alcohol

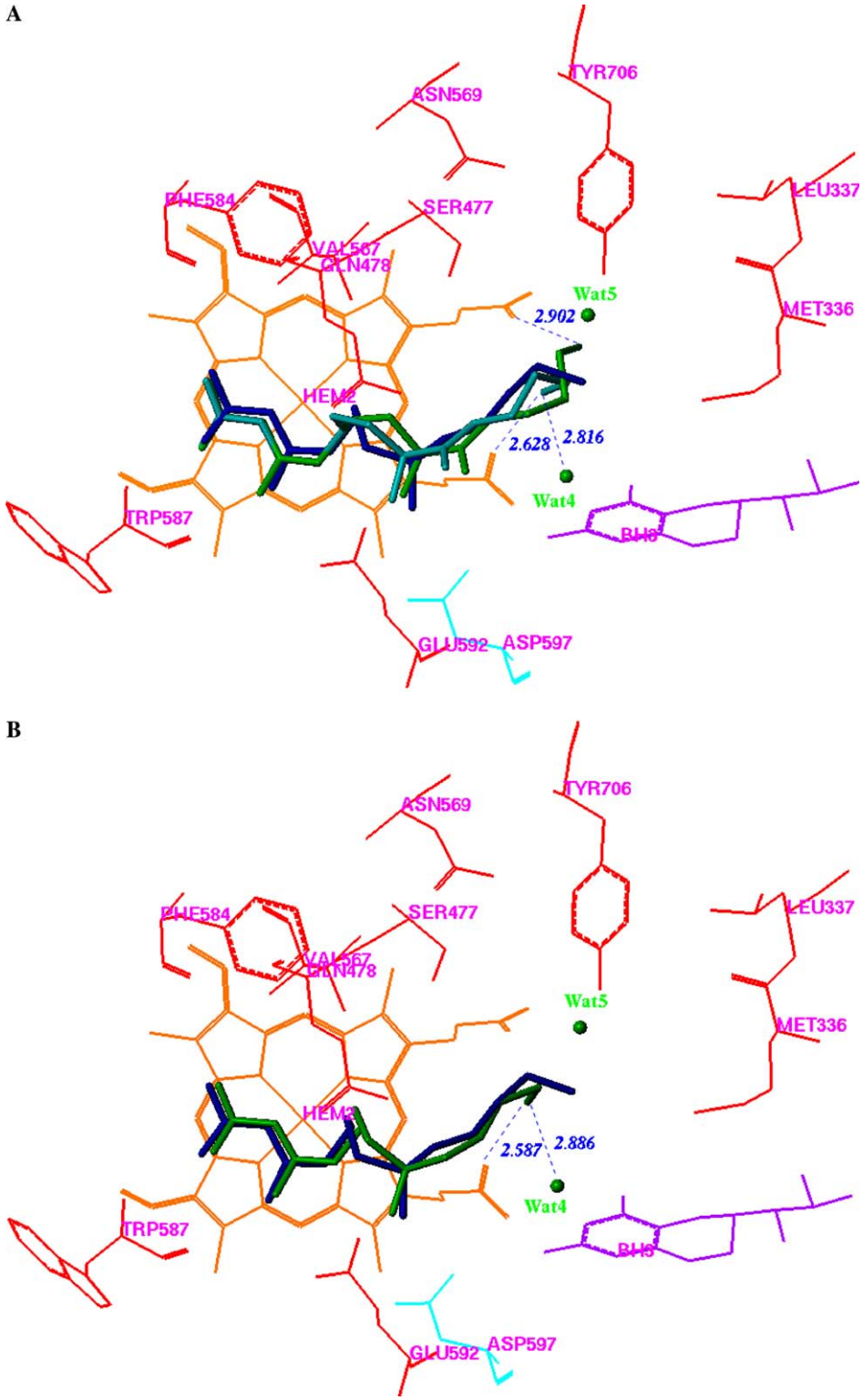

Figure 5. Docking results for **12** and **18** with nNOS. (A) The blue molecule is the crystallographic binding conformation of **4**. The green and cyan molecules are two different docking conformations of **12** with nNOS. None of the hydrogen atoms, except the one attached to the terminal oxygen atom of **12**, is shown. (B) The blue molecule is the crystallographic binding conformation of **4**; the green molecule is the docking conformation of **18** with nNOS. None of the hydrogen atoms is shown.

followed by DIEA to a solution of EDC, HOBt, and Boc-Arg^{NO_2}-OH in DMF at 0 °C. The reaction solution was allowed to gradually warm to ambient temperature, and stirring was continued for 12 h. After removal of the solvent by rotary evaporation, the residue was purified by column chromatography with 100% CH_2Cl_2 then 95/5 CH_2Cl_2/MeOH. In the case of **8**, a white solid precipitated from the reaction solution, which was filtered

off prior to column chromatography. Each amide product was isolated as a white solid, which showed a single spot with R_f 0.2 upon TLC analysis with 95/5 CH_2Cl_2/MeOH as eluent. Removal of the Boc groups was readily accomplished by overnight treatment of the protected amides with 8 mL of a 50% TFA/CH_2Cl_2 solution. After removal of CH_2Cl_2 and TFA under reduced pressure, the resulting residue was dissolved in distilled water and washed with EtOAc. Purification of the deprotected products (**11**–**13**) using reversed-phase preparative HPLC as described in Section 5.1 was carried out prior to conducting the assays.

5.4. (4*S*)-4-*N*-*tert*-Butoxycarbonylamino-5-(2-hydroxyethyl)amidopentyl-*N*-nitroguanidine (8)

Prepared as described in the general procedure with EDC (0.61 g, 3.18 mmol), HOBt (0.46 g, 3.40 mmol), Boc-Arg^{NO_2}-OH (1.03 g, 3.22 mmol), ethanolamine (0.2 mL, 3.31 mmol), and DIEA (0.7 mL, 4.02 mmol) in DMF (10 mL). ^{1}H NMR (500 MHz, CD_3OD) δ 4.08 (m, 1H), 3.60 (m, 2H), 3.34 (m, 4H), 3.28 (m, 2H), 1.66–1.81 (m, 4H), 1.43 (br s 9H). LRMS (ES^+): calcd ($M+H^+$):363.2; obsd: 363.0.

5.5. (4*S*)-*N*-(4-amino-5-[2-hydroxyethyl]amidopentyl)-*N*-nitroguanidine (11)

Removal of the Boc group of **8** as in the general procedure yielded 1.10 g (95% for two steps from Boc-Arg (NO_2)-OH) of **11**. t_R = 15.3 min; ^{1}H NMR (500 MHz, D_2O) δ 3.86 (t, J = 6.5, 1H), 3.50 (m, 2H), 3.23 (t, J = 5.5 Hz, 2H), 3.16 (m, 2H), 1.77 (m, 2H), 1.53 (m, 2H); ^{13}C NMR (500 MHz, D_2O) δ 163.0, 159.0, 59.8, 53.1, 49.0, 41.7, 40.4, 28.1. HRMS (ES) (*m*/*z*): $M+H^+$ calcd for $C_8H_{19}N_6O_4$ 263.1468. Found 263.1476.

5.6. (4*S*)-4-*N*-*tert*-Butoxycarbonylamino-5-(3-hydroxypropyl)amidopentyl-*N*-nitroguanidine (9)

Prepared as described in the general procedure with EDC (0.60 g, 3.13 mmol), HOBt (0.47 g, 3.48 mmol), Boc-Arg^{NO_2}-OH (1.01 g, 3.16 mmol), 3-aminopropanol (0.25 mL, 3.27 mmol), and DIEA (0.7 mL, 4.02 mmol) in DMF (10 mL). ^{1}H NMR (500 MHz, CD_3OD) δ 4.13 (m, 1H), 3.69 (m, 2H), 3.40 (m, 4H), 3.36 (m, 2H), 1.73–1.88 (m, 6H), 1.5 (br s, 9H). LRMS (ES^+), *m*/*z* calcd. ($M+H^+$): 377.2. Found: 377.1.

5.7. (4*S*)-*N*-(4-amino-5-[3-hydroxypropyl]amidopentyl)-*N*-nitroguanidine (12)

Removal of the Boc group of **9** as in the general procedure yielded 0.431 g (36% for two steps from Boc-Arg (NO_2)-OH) of **12**. t_R = 15.5 min; ^{1}H NMR (400 MHz, D_2O) δ 4.01 (t, J = 5.2 Hz, 1H), 3.64 (t, J = 5.6 Hz, 2H), 3.34 (m, 4H), 1.95 (br s, 2H), 1.79 (m, 2H), 1.72 (m, 2H); ^{13}C NMR (400 MHz, D_2O) δ 162.9, 159.1, 59.4, 53.3, 47.3, 40.6, 36.8, 31.1, 28.4. HRMS (ES) (*m*/*z*): M+ H^+ calcd for $C_9H_{21}N_6O_4$ 277.1624. Found 277.1625. Anal. Calcd for $C_9H_{20}N_6O_4 \cdot TFA \cdot 0.08H_2O$: C, 33.73; H, 5.44; N, 21.45. Found: C, 33.72; H, 5.44; N, 21.12.

5.8. (4*S*)-4-*N*-*tert*-Butoxycarbonylamino-5-(4-hydroxybutyl)amidopentyl-*N*-nitroguanidine (10)

Prepared as described in the general procedure with EDC (0.61 g, 3.18 mmol), HOBt (0.47 g, 3.48 mmol), Boc-Arg^{NO_2}-OH (1.1 g, 3.45 mmol), 4-aminobutanol (0.3 mL, 3.45 mmol), and DIEA (0.7 mL, 4.02 mmol) in DMF (10 mL). ^{1}H NMR (500 MHz, CD_3OD) δ 4.09 (m, 1H), 3.60 (m, 2H), 3.37 (m, 4H), 3.31 (m, 2H), 1.59–1.81 (m, 8H), 1.45 (br s, 9H). LRMS (ES^+) *m*/*z* calcd ($M+H^+$): 391.2; obsd: 391.1.

5.9. (4*S*)-*N*-(4-amino-5-[4-hydroxybutyl]amidopentyl)-*N*-nitroguanidine (13)

Removal of the Boc group of **10** as in the general procedure yielded 0.355 g (26% for two steps from Boc-Arg (NO_2)-OH) of **13**. t_R = 15.5 min; ^{1}H NMR (500 MHz, D_2O) δ 3.78 (t, J = 5.5 Hz, 1H), 3.38 (s, 1H), 3.10 (m, 4H), 3.01 (m, 1H), 1.72 (br s, 2H), 1.48 (m, 4H), 1.33 (br s, 2H); ^{13}C NMR (500 MHz, D_2O) δ 162.8, 158.8, 61.3, 53.0, 47.3, 40.3, 39.4, 28.8, 28.1, 24.9. HRMS (ES) (*m*/*z*): $M+H^+$ calcd for $C_{10}H_{23}N_6O_4$ 291.1781. Found 291.1784.

5.10. General procedure for the reduced amide bond dipeptidomimetic analogs 18–20

The nitroargininal intermediate **14** was prepared as previously described.[10] The amine derivatives were prepared according to the following general procedure: To a mixture of Boc-nitroargininal, amino alcohol, and crushed/dried 4 Å molecular sieves stirring in methanol at ambient temperature under argon was added pyridine–borane complex. After being stirred overnight, the solvent was removed by rotary evaporation, and the residue was purified by column chromatography with CH_2Cl_2 then 98/2 MeOH/Et_3N as eluents. The appropriate fractions were combined, treated with decolorizing charcoal, filtered, and the charcoal washed with methanol. TLC with methanol as eluent showed a single spot in all three cases, R_f = 0.25. Deprotection of the Boc group was accomplished by stirring the amines with a freshly prepared 50% TFA/CH_2Cl_2 solution for 9 h. Following solvent removal, the residue was taken up in distilled water and washed with EtOAc. Purification of the deprotected products (**18**–**20**) using reversed-phase preparative HPLC as described in Section 5.1 was carried out prior to conducting the assays.

5.11. (4*S*)-4-*N*-*tert*-Butoxycarbonylamino-5-(2-hydroxyethyl)aminopentyl-*N*-nitroguanidine (15)

This was prepared as described in the general procedure using N^{α}-(*tert*-butoxycarbonyl)-L-nitroargininal (1.01 g, 3.33 mmol), molecular sieves (1.18 g), ethanolamine (0.25 mL, 4.14 mmol), and pyridine-borane complex (0.3 mL, 2.97 mmol). ^{1}H NMR (500 MHz, CD_3OD) δ 3.52 (m, 2H), 3.45 (t, J= 5 Hz, 1H), 3.19–3.13 (m, 4H), 2.59 (m, 2H), 2.50 (m, 2H), 1.44–1.51 (m, 2H), 1.3 (br s, 9H). LRMS (ES^+) *m*/*z* calcd ($M+H^+$): 349.2. Found: 349.2.

5.12. (4*S*)-*N*-(4-amino-5-[2-hydroxyethyl]aminopentyl)-*N*-nitroguanidine (18)

Removal of the Boc group of **15** as in the general procedure yielded 0.70 g (48% for two steps from N^{α}-(*tert*-butoxycarbonyl)-L-nitroargininal) of **18** as a TFA salt. t_R = 12.4 min; ^{1}H NMR (500 MHz, D_2O) δ 3.65 (t, J = 5.0 Hz, 2H), 3.54 (t, J = 5.5 Hz, 1H), 3.24 (s, 2H), 3.10 (m, 2H), 3.07 (m, 2H), 1.59 (m, 4H); ^{13}C NMR (500 MHz, D_2O) δ 158.8, 57.6, 56.5, 48.8, 48.6, 41.3, 40.4, 27.8. HRMS (ES) (*m*/*z*): M+H$^+$ calcd for $C_8H_{21}N_6O_3$ 249.1675. Found 249.1671.

5.13. (4*S*)-4-*N*-*tert*-Butoxycarbonylamino-5-(3-hydroxypropyl)aminopentyl-*N*-nitroguanidine (16)

This was prepared as described in the general procedure using N^{α}-(*tert*-butoxycarbonyl)-L-nitroargininal (1.01 g, 3.33 mmol), molecular sieves (1.04 g), 3-aminopropanol (0.3 mL, 3.92 mmol), and pyridine–borane complex (0.3 mL, 2.97 mmol). ^{1}H NMR (500 MHz, CD_3OD) δ 3.30 (m, 2H), 3.11 (m, 2H), 2.60–2.54 (m, 4H), 1.66–1.59 (m, H), 1.38 (br s, 9H). LRMS (ES$^+$) *m*/*z* calcd (M+H$^+$): 363.2. Found: 363.3.

5.14. (4*S*)-*N*-(4-amino-5-[3-hydroxypropyl]aminopentyl)-*N*-nitroguanidine (19)

Removal of the Boc group of **16** as in the general procedure yielded 0.39 g (26% for two steps from N^{α}-(*tert*-butoxycarbonyl)-L-nitroargininal) of **19** as a TFA salt. t_R = 13.4 min; ^{1}H NMR (500 MHz, D_2O) δ 3.52 (m, 3H), 3.22 (t, J= 6.0 Hz, 1H), 3.14 (s, 1H), 3.04 (m, 1H), 2.91 (m, 3H), 1.76 (t, J= 6.0 Hz, 2H), 1.70 (m, 4H). ^{13}C NMR (500 MHz, D_2O) δ 159.0, 59.1, 59.0, 49.0, 46.9, 42.4, 37.5, 29.2, 28.0. HRMS (ES) (*m*/*z*): M+H$^+$ calcd for $C_9H_{23}N_6O_3$ 263.1832. Found 263.1829.

5.15. (4*S*)-4-*N*-*tert*-Butoxycarbonylamino-5-(4-hydroxybutyl)aminopentyl-*N*-nitroguanidine (17)

This was prepared as described in the general procedure using N^{α}-(*tert*-butoxycarbonyl)-L-nitroargininal (1.08 g, 3.56 mmol), molecular sieves (1.18 g), 4-aminobutanol (0.4 mL, 4.60 mmol), and pyridine–borane complex (0.3 mL, 2.97 mmol). ^{1}H NMR (500 MHz, CD_3OD) δ 3.65 (m, 1H), 3.54 (m, 2H), 3.33–3.22 (m, 4H), 2.60–2.52 (m, 4H), 1.55 (m, 8H), 1.42 (m, 9H). LRMS (ES$^+$) *m*/*z* calcd (M+H$^+$): 377.2. Found: 377.1.

5.16. (4*S*)-*N*-(4-amino-5-[4-hydroxybutyl])aminopentyl-*N*-nitroguanidine (20)

Removal of the Boc group of **17** as in the general procedure yielded 0.66 g (39% for two steps from N^{α}-(*tert*-butoxycarbonyl)-L-nitroargininal) of **20** as a TFA salt. t_R = 13.9 min; ^{1}H NMR (500 MHz, D_2O) δ 3.52 (t, J = 6.5 Hz, 1H), 3.41 (t, J = 6.0 Hz, 2H), 3.20 (m, 2H), 2.96 (m, 2H), 1.65 (m, 2H), 1.57 (m, 4H), 1.41 (m, 2H);^{13}C NMR (500 MHz, D_2O) δ 159.0, 61.0, 60.9, 48.8, 48.7, 48.6, 40.5, 28.4, 27.8, 22.4. HRMS (ES) (*m*/*z*): M+H$^+$ calcd for $C_{10}H_{25}N_6O_3$ 277.1988. Found 277.1990.

5.17. Enzyme preparation and assay

All three NOS isoforms used were recombinant enzymes overexpressed in *Escherichia coli* from different sources; there is very high sequence identity for the isoforms from different sources. nNOS was purified as previously described.[19] Bovine eNOS was prepared as previously reported[20]; murine macrophage iNOS was expressed and isolated according to the procedure of Hevel et al.[21] Nitric oxide formation was monitored by the hemoglobin capture assay as reported.[22]

5.18. Determination of K_i values

The apparent K_i values were obtained by measuring percent inhibition in the presence of 10 μM L-arginine with at least three concentrations of inhibitor. The parameters of the following inhibition equation[23] were fitted to the initial velocity data: % inhibition = 100[I]/{[I] + K_i(1 + [S]/K_m)}. K_m values for L-arginine were 1.3 μM (nNOS), 8.2 μM (iNOS), and 1.7 μM (eNOS). The selectivity of an inhibitor was defined as the ratio of the respective K_i values.

Acknowledgments

We are grateful to the National Institutes of Health (GM 49725 to R.B.S., T32 AG00260 through the Northwestern University Center for Drug Discovery and Chemical Biology to B.N.A.M, and GM52419 and HL30050 to Prof. Bettie Sue Masters, in whose laboratory P.M., L.J.R., and T.M.S. work) for financial support of this work.

References and notes

1. Stuehr, D. J.; Griffith, O. W. *Adv. Enzymol. Relat. Areas Mol. Biol.* **1992**, *65*, 287–346.
2. Kerwin, J. F., Jr.; Lancaster, J. R., Jr.; Feldman, P. L. *J. Med. Chem.* **1995**, *38*, 4342–4362.
3. Huang, H.; Lee, Y.; Zhang, H. Q.; Fast, W.; Riley, B.; Silverman, R. B. *R. Soc. Chem.* **2001**, *264*, 303–328 (Medicinal Chemistry into the Millenium).
4. Marletta, M. A. *J. Med. Chem.* **1994**, *37*, 1899–1907.
5. Erdal, E. P.; Litzinger, E. A.; Seo, J.; Zhu, Y.; Ji, H.; Silverman, R. B. *Curr. Top. Med. Chem.* **2005**, *5*, 603–624.
6. Silverman, R. B.; Huang, H.; Marletta, M. A.; Martásek, P. *J. Med. Chem.* **1997**, *40*, 2813–2817.
7. Huang, H.; Martásek, P.; Roman, L. J.; Silverman, R. B. *J. Med. Chem.* **2000**, *43*, 2938–2945.
8. Huang, H.; Martásek, P.; Roman, L. J.; Masters, B. S. S.; Silverman, R. B. *J. Med. Chem.* **1999**, *42*, 3147–3153.
9. Gomez-Vidal, J. A.; Martásek, P.; Roman, L. J.; Silverman, R. B. *J. Med. Chem.* **2004**, *47*, 703–710.
10. Hah, J.; Roman, L. J.; Martasek, P.; Silverman, R. B. *J. Med. Chem.* **2001**, *44*, 2667–2670.
11. Flinspach, M. L.; Li, H.; Jamal, J.; Yang, W.; Huang, H.; Hah, J.-M.; Gomez-Vidal, J.; Litzinger, E. A.; Silverman, R. B.; Poulos, T. L. *Nat. Struct. Mol. Biol.* **2004**, *11*(1), 54–59.

12. Flinspach, M.; Li, H.; Jamal, J.; Yang, W.; Huang, H.; Silverman, R. B.; Poulos, T. L. *Biochemistry* **2004**, *43*, 5181–5187.
13. Ji, H.; Li, H.; Flinspach, M.; Poulos, T. L.; Silverman, R. B. *J. Med. Chem.* **2003**, *46*, 5700–5711.
14. Gasteiger, J.; Marsili, M. *Tetrahedron* **1980**, *36*, 3219–3228.
15. ACD/log D suite, Advanced Chemistry Development Inc. Toronto, Canada (http://www.acdlabs.com).
16. Bomann, M. D.; Guch, I. C.; DiMare, M. *J. Org. Chem.* **1995**, *60*(18), 5995–5996.
17. Dunitz, J. D. *Science* **1994**, *264*, 670.
18. Lam, P. Y. S.; Jadhav, P. K.; Eyermann, C. J.; Hodge, C. N.; Ru, Y.; Bacheler, L. T.; Meek, J. L.; Otto, M. J.; Rayner, M. M.; Wong, Y. N.; Chang, C.-H.; Weber, P. C.; Jackson, D. A.; Sharpe, T. R.; Erickson-Viitanen, S. *Science* **1994**, *263*, 380–384.
19. Roman, L. J.; Sheta, E. A.; Martásek, P.; Gross, S. S.; Liu, Q.; Masters, B. S. S. *Proc. Natl. Acad. Sci. U.S.A.* **1995**, *92*, 8428–8432.
20. Martásek, P.; Liu, Q.; Roman, L. J.; Gross, S. S.; Sessa, W. C.; Masters, B. S. S. *Biochem. Biophys. Res. Commun.* **1996**, *219*, 359–365.
21. Hevel, J. M.; White, K. A.; Marletta, M. *J. Biol. Chem.* **1991**, *266*, 22789–22791.
22. Hevel, J. M.; Marletta, M. *Methods Enzymol.* **1994**, *133*, 250–258.
23. Segel, I. H. *Enzyme Kinetics*; John Wiley: New York, 1975, p 105.